Vortex ring formation at tube and orifice openings

D. I. Pullin

Department of Mechanical Engineering, University of Melbourne, Parkville, Victoria, 3052, Australia
(Received 12 June 1978)

The formation, at tube and orifice openings, of vortex rings generated by a piston moving with velocity proportional to time to some power m, is considered. The expansion of the axisymmetric generating flow about the circular forming edge is used in conjunction with the similarity theory of edge vortex growth to model the ring formation process. For large Reynolds numbers the ring diameter and circulation are not strongly dependent on the piston velocity profile. However, the ring viscous subcore shows peaks in the tangential velocity profile only if $m < (\pi-\theta_e)/(2\pi-\theta_e)$, where θ_e is the edge forming angle.

I. INTRODUCTION

In a recent paper, Saffman[1] discussed the process of vortex ring formation at sharp-edged tube and orifice openings utilizing a similarity theory of the formation of a vortex at a sharp edge in an impulsively started flow. He obtained estimates of the ring diameter and circulation which were in fair agreement with the measurements of Liess and Didden[2] and Maxworthy[3] even though it was assumed that the flow generating the vortex ring was two dimensional. It is the purpose of the present paper to extend this model to properly account for the axisymmetric geometry of the ring forming apparatus, and also to include a class of generating flow piston movements other than impulsive motion.

We consider vortex rings formed by the movement of a piston of diameter D_p in a cylinder with either a tube or orifice type ring-forming opening of diameter D as shown in Fig. 1. The piston moves through a short distance or stroke

$$\bar{L} = \int_0^{t_f} U_p(t)\,dt\,, \tag{1}$$

$$U_p(t) = A_p t^m\,, \tag{2}$$

where t_f is the piston movement or ring formation time, $U_p(t)$ is the piston velocity profile, and $m \geq 0$ and A_p are constants. The impulsive case is given by $m = 0$ while for all m the piston is assumed to stop impulsively at $t = t_f$. The average piston speed $\bar{U}_p$ in $(0, t_f)$ is given by

$$A_p = (1+m)\,\bar{U}_p^{1+m}\bar{L}^{-m}\,. \tag{3}$$

The piston movement causes the boundary layer formed on the inner cylinder wall to separate at the opening and roll up into a toroidal vortex structure forming the vortex ring. For t_f small such that the scale of the forming vortex $r_I \ll D$, the flow near the opening may be considered to be locally two dimensional so that similarity theories of the vortex formation process[4-8] will provide a good model of the core of the vortex ring.

II. EFFECT OF GEOMETRY

The similarity theory vortex growth and circulation shedding rates are governed by constants in the leading order two-dimensional-like expansion of the attached or outer ring-generating flow near the sharp edge. Using polar coordinates r, θ near a two-dimensional sharp edge $\theta = \pi$, this expansion of the velocity potential takes the form $\phi = at^m r^{1/2}\sin(\theta/2)$ where the constant a is given by

$$a = K_1 A_p D^{1/2} \tag{4}$$

and K_1 is a dimensionless constant depending on the geometry of the apparatus. For the orifice geometry, a good model of the outer flow is the symmetrical potential flow through an orifice in an infinite flat plate. An exact solution for this problem is given by Lamb (Ref. 9, p. 138) from which the value $K_1 = 0.5\,(D_p/D)^2$ may be obtained. There appears to be no analytical solution for the tube geometry, but a numerical solution obtained by the author (Appendix) gives, to a good approximation, $K_1 = (2\pi)^{-1/2}$ compared with $(\pi)^{-1/2}$ for the corresponding two-dimensional channel.

III. CORE CIRCULATION AND DIAMETER

Assuming that the circulation in the ring Γ and the core radius r_I are those appropriate to the two-dimensional vortex shed in time t_f, then the similarity theory gives[8]

$$\Gamma = K_2\left[\frac{0.75\,a^4}{(1+m)}\right]^{1/3} t_f^{(4/3)(1+m)-1}\,, \tag{5}$$

$$r_I = K_3\left[\frac{0.75\,a}{(1+m)}\right]^{2/3} t_f^{(2/3)(1+m)}\,, \tag{6}$$

where K_2 and K_3 are dimensionless constants obtained

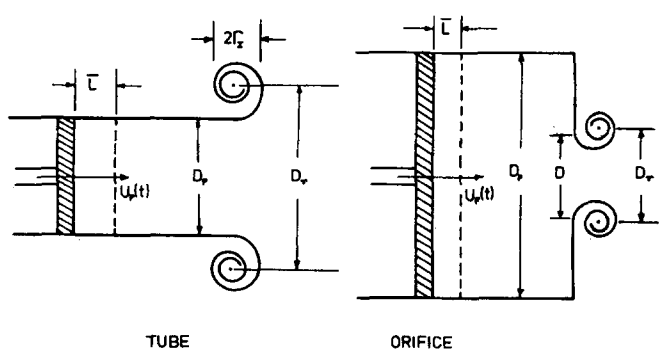

FIG. 1. Tube and orifice geometry for generation of vortex rings.

 0031-9171/79/030401-03$00.90

TABLE I. Values of the constant K_4.

m	Tube	Orifice
0	1.41	1.90
$\frac{1}{2}$	1.64	2.22
1	1.74	2.36

from similarity theory calculations. For Γ, defining the slug circulation[3] as

$$\Gamma_0 = \frac{1}{2}\int_0^{\bar{L}} U_p(L)\,dL \tag{7}$$

and using Eqs. (4) and (5), then

$$\frac{\Gamma}{\Gamma_0} = K_4(m, \text{geometry})\left(\frac{D_p}{D}\right)^2\left(\frac{\bar{L}}{D_p}\right)^{-2/3} . \tag{8}$$

Values of K_4 for different m and geometry, obtained from the author's[8] similarity calculations are given in Table I. The comparison for $m=0$ with the tube data of Maxworthy[3] in Fig. 2 is good for $\bar{L}/D_p = 1.6$, but worsens for higher $\bar{L}/D_p$. In the orifice apparatus experiments of Sallet[10] $\bar{L}/D_p = \frac{1}{3}$, $D_p/D = 2$, and $m=0$. For the three piston velocities $U_p = 1.41$, 1.27, and 0.98 m/sec used by Sallet, Eq. (8) gives $\Gamma = 0.4497$, 0.4047, and 0.3114 $m^2\,sec^{-1}$, respectively, compared with measured values of 0.6528, 0.5419, and 0.4322 $m^2\,sec^{-1}$, so that the comparison is only qualitatively reasonable.

Putting the ring diameter $D_r = D + 2r_I$ for the tube geometry and $D_r = D$ for the orifice (i.e., the center of the shed vortex moves approximately normal to the sharp edge), then Eq. (6) gives

$$D_r/D = 1 + K_5(\bar{L}/D)^{-2/3} , \tag{9}$$

where $K_5 = 0$ for the orifice and is a very weak function of m for the tube geometry. The estimate $K_5 = 0.32$ gives the curve which shows reasonable comparison with the data of Maxworthy[3] in Fig. 3. Useful estimates of values of $\bar{L}/D$ for which the similarity theory may be valid may be obtained by assuming $r_I \ll D/2$, yielding

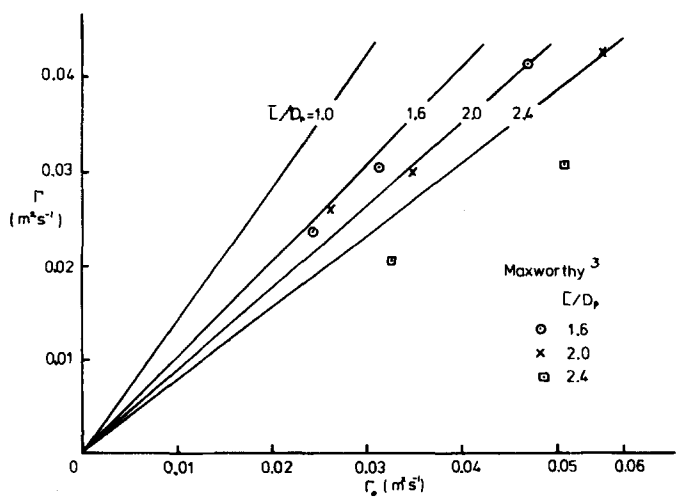

FIG. 2. Predicted ring circulation Γ [Eq. (8)] for $m=0$ compared with the tube data of Maxworthy.[3]

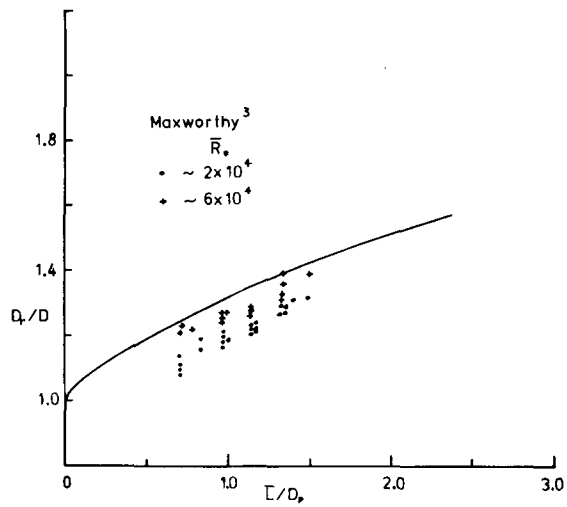

FIG. 3. Predicted ring diameter D_r/D [Eq. (9)] for $m=0$ compared with tube data of Maxworthy.[3]

$$\bar{L}/D_p \lesssim 4.7 , \tag{10a}$$

$$\bar{L}/D_p \lesssim 3.7/(D_p/D)^3 , \tag{10b}$$

for the tube and orifice geometries, respectively. These conditions are only approximately satisfied in experiments, which might explain some of the discrepancy between theory and measurement.

IV. CORE STRUCTURE

Here, we generalize the discussion to include a vortex ring formed at an edge of angle $\pi/2 \geq \theta_e \geq 0$ and define $\delta = \pi/(2\pi - \theta_e)$. In treating the spiral roll up of the plane vortex sheet shed by a rectangular wing, Moore and Saffman[11] show how the singular behavior of the velocity field near the spiral center is resolved by viscous action. The structure of the edge generated vortex may be obtained from Moore and Saffman's analysis (here, of course, axial velocity effects are absent), and results for $\delta = 0$, $m=0$ were given by Saffman.[1] Results for general δ, m follow by replacing Moore and Saffman's parameter n by $P = (2-\delta)/(1+m) - 1$. According to their model, the vortex core forming at the edge may be divided into three regions:

(i). A tightly wound spiral-like thin shear layer from the forming edge of radius $r_I \sim (\gamma t)^{1/(P+1)}$, γ being a constant.

(ii). A region in which the effects of decreasing spacing between shear layer turns (due to vortex sheet stretching) as $r^{2+P}t^{-1}$ and layer thickening as $(\nu t)^{1/2}$ due to viscous diffusion forms an essentially inviscid rotational core of radius $r_{II} \sim (\epsilon\nu^{1/2}t^{3/2})^{1/(2+P)}$. The smoothed out tangential velocity field in this region is[8]

$$v_\theta = \beta r^{-P} , \tag{11}$$

and ϵ and β are dimensional constants.

(iii). A viscous subcore of radius $r_{III} \sim (\nu t)^{1/2}$.

The ordering $r_I > r_{II} > r_{III}$ is preserved provided $t \gg t_\nu$ where $t_\nu = [\nu^{2-\delta}/\gamma^{2(1+m)}]^{1/(2m+\delta)}$ is the time at which inertial effects begin to dominate in region I of the vortex. For $\delta = \frac{1}{2}(\theta_e = 0)$ estimates of t_ν/t_f may be obtained in

terms of powers of $\bar{R}_e^{-1} = \nu/\bar{U}D[\bar{U} = (D_p/D)^2 \bar{U}_p]$ and $(\bar{L}/D)^{-1}$ which are proportional to $1/(2m+\delta)$. For common experimental values of $\bar{R}_e \sim 10^4$, $\bar{L}/D \sim 1$, $t_\nu/t_f \ll 1$ provided m is not much greater than unity. For larger m (which would be unlikely, in practice) viscous effects may be important for a longer portion of t_f, but the rapid growth of $r_{\rm I}$ as $t^{(1+m)/(2-\delta)}$ is finally telling. Putting $r_{\rm III} = (4\nu t)^{1/2}$, the ratio $r_{\rm I}/r_{\rm III}$ at $t = t_f$ may be obtained as

$$r_{\rm III}/r_{\rm I} = 2.8\bar{R}_e^{-1/2}(\bar{L}/D_p)^{-1/6}, \tag{12a}$$

$$r_{\rm III}/r_{\rm I} = 2.4\bar{R}_e^{-1/2}(D_p/D)^{-3/2}(\bar{L}/D_p)^{-1/6}, \tag{12b}$$

for the tube and orifice geometries, respectively (actually, the constants depend weakly on m) from which it follows that in most experimental situations the vortex ring is at least initially dominated by inertial effects for all m. After rupture from the edge, $t = t_f$, $r_{\rm III}$ will continue to increase at $(\nu t)^{1/2}$ while $r_{\rm I}$ should remain roughly constant. Assuming that vortex stretching of the shear layer ceases after rupture then $r_{\rm II}$ will continue to increase as $r_{\rm II} \sim (\nu t)^{1/2(P+2)}$ purely due to thickening of the shear layer.

The tangential velocity field in regions II and III is given by

$$v_\theta = \frac{\beta 2^{-P}\Gamma(\frac{3}{2} - \frac{1}{2}P)}{(\nu t)^{P/2}} M(\tfrac{1}{2} + \tfrac{1}{2}P, 2, \eta), \tag{13}$$

where $\eta = -r^2/4\nu t$, r is the distance from the vortex center, M is the hypergeometric function, and Eq. (13) smoothly matches Eq. (11) for large r. For $m < 1 - \delta$, which corresponds to the singular behavior of Eq. (11) as $r \to 0$, there is a maximum in the velocity field given by Eq. (13). For $m > 1 - \delta$, there is no v_θ maximum in region III so that $(v_\theta)_{\max}$ will occur somewhere on the outer turns of the thin shear-layer structure in region I. The vorticity distribution which may be obtained from Eq. (13) peaks at $r = 0$ for all m, δ with maximum value

$$\omega_{\max} = \beta 2^{-P}\Gamma(\tfrac{3}{2} - \tfrac{1}{2}P)(\nu t)^{-(P+1)/2}.$$

Unfortunately, comparison of vorticity profiles with the measurements of Maxworthy[3] is difficult since insufficient data are given.

APPENDIX: GENERATING FLOW FOR TUBE GEOMETRY

For the tube geometry we use the model of axisymmetric incompressible potential flow of a rate $A_p t^m \pi D^2/4$ from a semi-infinite circular tube of radius $R = D/2$, $x \le 0$. This problem may be formulated by regarding the tube as a fixed cylindrical vortex sheet of strength $\gamma(x)$, $x \le 0$. Using standard results (Ref. 9, p. 237) for an axisymmetric vortex system, an integral equation for γ may be then obtained as

$$\pi = \int_{-\infty}^{0} \hat{\gamma}(u)\, G(u_0, u)\, du, \quad u_0 \le 0 \tag{A1}$$

where

$$\hat{\gamma} = \gamma/A_p t^m, \quad u = 2x/D$$

$$G(u_0, u) = (\rho_1 + \rho_2)[K(\lambda) - E(\lambda)],$$

$$\rho_1 = [(u - u_0)^2 + 4]^{1/2}, \quad \rho_2 = |u_0 - u|,$$

$$\lambda = \left(\frac{\rho_1 - \rho_2}{\rho_1 + \rho_2}\right)^2,$$

and $K(\lambda)$ and $E(\lambda)$ are complete elliptic integrals of the first and second kind, respectively. For large $|u|$, a source approximation leads to $\gamma \sim 1 + 1/4u^2 + \ldots$ while for small $|u|$ it may be shown that $\gamma \sim \sqrt{2}K_1|u|^{-1/2}$ where K_1 is as in Eq. (4). Introducing $v = (-u)^{1/2}$, $f = v\gamma$ in Eq. (A1) leads to an equation for $f(v)$ with $f(0) = \sqrt{2}K_1$ and $f(v) \sim v + v^{-3}/4 + \ldots$ for large v.

For v greater than some value v_c, the large v solution was assumed valid while in $(0, v_c)$ a numerical solution to Eq. (A1) in f-v space was obtained by transforming the integral equation into a set of 64 linear equations using 64 point Gaussian quadrature in $(0, v_c)$ together with appropriate treatment of the logarithmic singularity in G near $v = v_0$.

For $v_0 = \sqrt{3}$ and 3, the method was tested by computing the equivalent two-dimensional problem, and also the orifice flow problem. In both cases the numerical solutions agreed with the exact solutions to better than 1 in 10^3 at all points except very near $v = v_c$. The values of K_1 were 0.564173 and 0.4998 compared with the exact values of $\pi^{-1/2}$ and 0.5, respectively. For the tube problem $K_1 = 0.398939$ compared with $(2\pi)^{-1/2} = 0.398942\ldots$ which perhaps indicates that this value is exact!

[1] P. G. Saffman, J. Fluid Mech. **84**, 625 (1978).
[2] C. Liess and N. Didden, Z. Angew. Math. Mech. **56**, T206 (1976).
[3] T. Maxworthy, J. Fluid Mech. **81**, 465 (1977).
[4] L. Anton, Ing. Arch. **10**, 411 (1939).
[5] E. Wedemeyer, Ing. Arch. **30**, 187 (1961).
[6] N. Rott, J. Fluid Mech. **1**, 111 (1956).
[7] W. Blendermann, Schiffstechnik **16**, 3 (1969).
[8] D. I. Pullin, J. Fluid Mech. **88**, 401 (1978).
[9] H. Lamb, *Hydrodynamics* (Dover, New York, 1932), p. 138.
[10] D. W. Sallet, Phys. Fluids **18**, 109 (1975).
[11] D. W. Moore and P. G. Saffmann, Proc. R. Soc. London Ser. A **333**, 491 (1973).